

Energy transfer in resonant and near-resonant internal wave triads for weakly non-uniform stratifications

G. Saranraj¹ and Anirban Guha^{1,2†}

¹Environmental and Geophysical Fluids Group, Department of Mechanical Engineering, Indian Institute of Technology, Kanpur, U.P. 208016, India.

²Institute of Coastal Research, Helmholtz-Zentrum Geesthacht, Geesthacht 21502, Germany.

(Received xx; revised xx; accepted xx)

In this paper, we derive a simplified mathematical model for calculating the energy exchange in resonant and near-resonant triads consisting of weakly nonlinear internal gravity wave packets in weakly non-uniform density stratifications. Such triad interactions are one of the mechanisms by which high wavenumber internal waves lead to ocean turbulence and mixing via parametric subharmonic instability (PSI). We assume each internal wave to have a slowly varying amplitude and a rapidly varying phase (both in space and time), and derive the amplitude evolution equations using the method of multiple scales. It is shown that, although the ‘pump-wave approximation’ of PSI using the normal mode forms for a near-resonant triad predict the initial growth rates accurately, it fails to provide the complete picture of energy transfer between the wave packets. We observe that each near-resonant wave packet in a triad has to be of larger size in comparison to a resonant wave packet (of the same wavenumber and frequency) to exchange the same percentage of energy. Energy transfer in non-uniform stratification introduces wave detuning, which may strongly affect the energy transfer process. Also, when wave packets forming a triad move to a higher (lower) stratification from the base stratification where the triad conditions are perfectly met, the group speed of the packets decrease (increase) and the non-linear coupling coefficients increase (decrease). For waves packets with frequencies $\omega \approx N$, where N is the buoyancy frequency, even a small change in N can cause a significant mismatch in the vertical wavenumbers. This results in a sharp reduction in the growth rates of the wave packets. For wave packets satisfying $\omega \ll N$, the vertical wavenumbers of the wave packets are almost a linear function of N . Therefore, when wave packets forming a triad move to a higher stratification, the effect of the vertical wavenumber mismatch is less in comparison to the reduced group speed or increased non-linear coefficients. This results in increased growth rates. It is also shown that the energy transfer process between the wave packets of a resonant triad in a uniform stratification can be significantly different from the case of a weakly varying stratification, provided all wave packets have nearly same order of magnitude of energy.

Key words: Internal gravity waves, wave triads, nonlinear density stratification, parametric subharmonic instability

† Email address for correspondence: anirbanguha.ubc@gmail.com

1. Introduction

Internal gravity waves are often produced in the oceans when the stably stratified ocean water is driven back and forth over submarine topography by tidal currents. Low-mode internal gravity waves have long wavelengths, and can travel long distances from their generation site without dissipation (St. Laurent & Garrett 2002). Understanding the mechanism(s) behind the breakdown of these waves is an active area of research, since it finally leads to small scale ocean mixing. One of the plausible mechanisms through which this breakdown occurs is ‘parametric subharmonic instability’ (PSI) – a nonlinear interaction between waves forming a resonant triad by which energy is transferred from low wavenumber, high frequency modes to high wavenumber, low frequency modes (Miles 1978). In a resonant internal gravity wave triad, a primary (or parent) wave of angular frequency ω_1 and wavevector \mathbf{k}_1 resonantly forces two ‘daughter’ waves by transferring its own energy, when both the conditions $\omega_1 = \omega_2 + \omega_3$ and $\mathbf{k}_1 = \mathbf{k}_2 + \mathbf{k}_3$ are met (Craig 1988). For a given primary wave, it is possible to have multiple daughter waves satisfying the resonant triad condition.

From laboratory experiments and theoretical analyses, Bourget *et al.* (2013) showed that in a uniformly stratified fluid, the growth rate of the daughter waves depends on the wavenumber, angular frequency and Reynolds number of the primary wave. Since ocean’s density stratification is non-uniform, recent efforts have been directed towards understanding energy transfer in non-uniformly stratified fluids. Triads in non-uniform stratification behave differently because of the wavenumbers’ dependence on stratification. Monochromatic internal gravity waves are an exact solution to the fully nonlinear Navier-Stokes equation in a uniformly stratified fluid (Lighthill & Lighthill 2001). The same is not true when the fluid is non-uniformly stratified; moreover, a given mode can interact with itself. Through such self interaction, a parent mode in a non-uniform stratification can yield superharmonic daughter modes having twice of the parent’s horizontal wavenumber (Sutherland 2016). However, Sutherland (2016) didn’t find any occurrence of PSI. Diamessis *et al.* (2014) showed that superharmonics mainly form when the pycnocline is sharp. Similar conclusions were obtained in Gayen & Sarkar (2013); they showed that the energy transfer through PSI is negligible when the primary waves have vertical wavelength comparable to the pycnocline thickness. However, significant energy transfer through PSI is observed when the vertical wavelength of the waves are nearly an order of magnitude lesser than the pycnocline thickness. Using a weakly nonlinear analysis, Wunsch (2017) studied the self interaction of a low mode internal gravity wave assuming the stratification to be layerwise constant, and found that self-interaction of a primary mode can resonantly force superharmonic waves, similar to what was concluded in Sutherland (2016). Varma & Mathur (2017) provided the necessary conditions for a mode to resonantly force other modes (through self interaction or by interaction with other modes) in a general non-uniform stratification using weakly nonlinear analysis. From these previous studies, it can be inferred that the length scale of stratification plays a key role in determining the cascading process of the primary mode, that is, whether it will be superharmonic or subharmonic.

In this paper, we have focused on internal wave triads whose constituent waves have vertical wavelengths at least an order of magnitude less than the pycnocline’s thickness. We have considered *broad* pycnoclines with typical width of $\mathcal{O}(100\text{ m})$. Such pycnoclines have been considered in Grisouard *et al.* (2011) for studying solitary wave generation in the Bay of Biscay. Mathur *et al.* (2016) have also considered such broad pycnoclines while investigating internal gravity waves generation due to oscillating barotropic flow over a topography. In such scenario, the vertical wavenumber of the internal waves

undergo a slow variation in space, unlike what happens in rapidly varying stratification. Furthermore, higher modes are far less studied, they can lead to small scale turbulence and mixing via PSI type triad interactions (St. Laurent & Garrett 2002). Energy flux estimation in the Mid-Atlantic Ridge has revealed that high modes (e.g. modes 10–25) contain about 18% of the total flux (St. Laurent & Garrett 2002; St. Laurent & Nash 2004). Additionally, internal beams having higher modes are also not uncommon in oceans. For example, M_2 internal gravity wave beams composed of high wavenumbers (expected to more than mode 100) have been observed in the seismic images of the Norwegian sea (Holbrook *et al.* 2009).

In addition to perfect triads, we have also focused on near-resonant triads, that is, waves which *almost* satisfy the triad condition. Such triads have previously been studied by Lamb (2007); it was shown that near-resonant triads can occur when internal gravity waves generated via tide-topography interactions interact among themselves. The interaction strength was also found to be comparable to that of an exact triad. Near-resonant wave packet (i.e., finite width) triads have also been studied for gravity waves in compressible atmosphere, see Huang *et al.* (2007). In this situation, near-resonance comes from a frequency mismatch instead of wavenumber mismatch. We also note that such near resonant triads are also observed in other branches of physics. For example, Chu & Scott (1975) studied near-resonant triads occurring in Raman scattering using Inverse scattering transform.

The paper is organized as follows. In §2, we derive the amplitude evolution equations of the constituent waves of a resonant triad (hereafter, the word ‘resonant’ is often omitted for simplicity). To obtain these equations, we have reduced the inviscid, incompressible, two-dimensional (2D) Boussinesq Navier-Stokes equations by assuming the streamfunction and the corresponding buoyancy perturbation due to each wave to be a product of slowly varying amplitude and rapidly varying phase. In §3, we focus on the effect of the group speed in triad interactions for infinitely wide waves. Also, we study the energy transfer between near-resonant finite width wave packets in uniform stratification and varying stratification. In §4 we study the energy transfer between near-resonant wave packets that are localised in space, as well as the energy exchange between wave packets in the presence of varying stratification. The paper is summarized and concluded in §5.

2. Derivation of the governing equations

The inviscid, incompressible, 2D (in the x - z plane) Boussinesq Navier-Stokes equations, in the absence of a background flow, can be compactly written in terms of the perturbation streamfunction ψ and the perturbation buoyancy b as follows:

$$\frac{\partial}{\partial t} (\nabla^2 \psi) = -\{\nabla^2 \psi, \psi\} - \frac{\partial b}{\partial x}, \quad (2.1a)$$

$$\frac{\partial b}{\partial t} - N^2(\epsilon_n z) \frac{\partial \psi}{\partial x} = -\{b, \psi\}. \quad (2.1b)$$

Here $N^2 \equiv -(g/\rho^*) (d\bar{\rho}/dz)$ is the squared buoyancy frequency, $\bar{\rho}$ is the base density profile and ρ^* is the reference density. The perturbation buoyancy is defined as $b = -g\rho/\rho^*$, where ρ is the perturbation density. The buoyancy frequency is assumed to vary *weakly* with z , the parameter ϵ_n , defined in (2.7), provides a quantitative measure of this weak variation. The Poisson bracket is defined as $\{G_1, G_2\} \equiv (\partial G_1/\partial x)(\partial G_2/\partial z) - (\partial G_1/\partial z)(\partial G_2/\partial x)$. The physics is expected to be qualitatively similar if we consider the problem in 3D, hence for simplification we have restricted our analyses to 2D. The Coriolis

effect has also been neglected since it would not change the results qualitatively. Viscosity is also neglected because in the scale of the waves we use for the triad interaction, diffusion is expected to play a very minor role.

Instead of solving the fully nonlinear equations (2.1a)–(2.1b) numerically, we combine (2.1a) and (2.1b) into a single equation and employ a multiple scale analysis. In this regard we perform $\partial(2.1a)/\partial t - \partial(2.1b)/\partial x$, which results in

$$\frac{\partial^2}{\partial t^2} (\nabla^2 \psi) + N^2(\epsilon_n z) \frac{\partial^2 \psi}{\partial x^2} = -\frac{\partial}{\partial t} (\{\nabla^2 \psi, \psi\}) + \frac{\partial}{\partial x} (\{b, \psi\}). \quad (2.2)$$

For performing multiple scale analysis, we assume wavelike perturbations, and the streamfunction due to the j -th wave ($j = 1, 2, 3$ since we will be considering a wave-triad) is given according to the following ansatz:

$$\psi_j = \epsilon_a a_j(\epsilon_z z, \epsilon_x x, \epsilon_t t) F_j(z) e^{i(k_j x - \omega_j t)} + \text{c.c.}, \quad (2.3)$$

where ‘c.c.’ denotes the complex conjugate, a_j is the slowly varying complex amplitude, k_j is the horizontal wavenumber and ω_j is the angular frequency of the j -th wave. $F_j(z)$ is the vertical structure of a j -th wave. Similar to ϵ_n , small parameters ϵ_t , ϵ_x and ϵ_z are respectively used to denote the weak variation of the amplitude function with time, streamwise (x) direction and z direction. The small parameter ϵ_a is used to signify the amplitude of the wave. Scaling analysis to find the relations between these small parameters is given in Appendix A.

The buoyancy perturbation, corresponding to the streamfunction assumed in (2.3), at the leading order ($\mathcal{O}(\epsilon_a)$) is given by:

$$b_j = -\epsilon_a \frac{N^2(\epsilon_n z) k_j}{\omega_j} a_j(\epsilon_z z, \epsilon_x x, \epsilon_t t) F_j(z) e^{i(k_j x - \omega_j t)} + \text{c.c.} \quad (2.4)$$

The above expression is obtained if the streamfunction expression in (2.3) is substituted in (2.1a). We note that this is very similar to the procedure of obtaining buoyancy perturbation through polarization relation; see Bourget *et al.* (2013). The streamfunction (2.3) and the buoyancy perturbation (2.4) ansatzes are substituted in (2.2). At leading order ($\mathcal{O}(\epsilon_a)$), the governing equation reduces to an eigenvalue problem

$$\frac{d^2 F_j}{dz^2} + k_j^2 \left(\frac{N^2(\epsilon_n z)}{\omega_j^2} - 1 \right) F_j = 0, \quad (2.5)$$

solving which we can obtain the vertical structure $F_j(z)$ of the j -th wave. For weakly varying stratification, we can use the Wentzel–Kramers–Brillouin (WKB) method and solve (2.5). The solution for F_j up to the second order accuracy, is given by

$$F_j = \frac{1}{\sqrt{m_j}} e^{i \int_0^z m_j dz}, \quad (2.6)$$

where $m_j(\epsilon_z z) = k_j \sqrt{N^2(\epsilon_n z)/\omega_j^2 - 1}$ is the vertical wavenumber. We observe here that m_j varies with a variation in N . The quantity ϵ_n is defined as

$$\epsilon_n \equiv \max \left(\frac{1}{Nm_3} \frac{dN}{dz} \right), \quad (2.7)$$

where m_3 is the vertical wavenumber of wave ‘3’. This is the wave which is used as the primary wave in all the simulations. The quantity ϵ_z is defined as:

$$\epsilon_z \equiv \max \left(\epsilon_n, \frac{\Delta m}{m_3} \right), \quad (2.8)$$

where $\Delta m = m_1 + m_2 - m_3$ at any location in space. We have used separate small parameters for the variation of amplitude in the z -direction and the buoyancy frequency. This is because they can be independent of each other. For example, near-resonant triads with vertical wavenumber mismatch can occur even in a uniform stratification ($\epsilon_n = 0$), but the amplitude of the waves will still vary in space ($\epsilon_z \neq 0$). At the leading order ($\mathcal{O}(\epsilon_a)$), the waves satisfy the dispersion relation and behaves as a linear wave. However, at the next order ($\mathcal{O}(\epsilon^2)$), that is, terms such as ($\mathcal{O}(\epsilon_a \epsilon_z)$), ($\mathcal{O}(\epsilon_a \epsilon_t)$), ($\mathcal{O}(\epsilon_a \epsilon_x)$), ($\mathcal{O}(\epsilon_a^2)$), triad interactions (through the nonlinear terms) slowly modulate the amplitude of each constituent wave. To study the triad interactions between the waves, the $\mathcal{O}(\epsilon^2)$ terms are gathered after substituting the streamfunction (2.3) and the buoyancy perturbation (2.4) ansatzes in (2.2). For convenience, we define the phase part as $\mathfrak{P}_j \equiv F_j(z)e^{i(k_j x - \omega_j t)}$. The LHS is then given by:

$$\begin{aligned} \text{LHS} &= \sum_{j=1}^3 \frac{\partial^2 (\nabla^2 (\epsilon_a a_j \mathfrak{P}_j))}{\partial t^2} + N^2(\epsilon_n z) \frac{\partial^2 (\epsilon_a a_j \mathfrak{P}_j)}{\partial x^2} + \text{c.c} \\ &= \sum_{j=1}^3 2i\epsilon_a \left(-\epsilon_z m_j \omega_j^2 \frac{\partial a_j}{\partial(\epsilon_z z)} + \epsilon_t (k_j^2 + m_j^2) \omega_j \frac{\partial a_j}{\partial(\epsilon_t t)} + \epsilon_x k_j (N^2(\epsilon_n z) - \omega_j^2) \frac{\partial a_j}{\partial(\epsilon_x x)} \right) \mathfrak{P}_j \\ &\quad + \text{c.c.} \end{aligned} \tag{2.9}$$

The first term of the RHS is

$$\begin{aligned} -\frac{\partial (\{\nabla^2 \psi, \psi\})}{\partial t} &= (\omega_1 + \omega_2) a_1 a_2 ((k_1 m_2 - k_2 m_1) (m_2^2 + k_2^2 - k_1^2 - m_1^2)) e^{i(k_3 x - \omega_3 t)} F_1 F_2 \\ &\quad + (\omega_3 - \omega_2) a_3 \bar{a}_2 ((k_3 m_2 - k_2 m_3) (m_3^2 + k_3^2 - k_2^2 - m_2^2)) e^{i(k_1 x - \omega_1 t)} F_3 \bar{F}_2 \\ &\quad + (\omega_3 - \omega_1) a_3 \bar{a}_1 ((k_3 m_1 - k_1 m_3) (m_3^2 + k_3^2 - k_1^2 - m_1^2)) e^{i(k_2 x - \omega_2 t)} F_3 \bar{F}_1 + \text{c.c.}, \end{aligned}$$

while the second term is given by

$$\begin{aligned} \frac{\partial (\{b, \psi\})}{\partial x} &= N^2(k_1 + k_2) a_1 a_2 \left(\frac{k_1^2 m_2}{\omega_1} + \frac{k_2^2 m_1}{\omega_2} - \frac{k_1 k_2 m_2}{\omega_2} - \frac{k_1 k_2 m_1}{\omega_1} \right) e^{i(k_3 x - \omega_3 t)} F_1 F_2 \\ &\quad + N^2(k_3 - k_2) a_3 \bar{a}_2 \left(-\frac{k_3^2 m_2}{\omega_3} - \frac{k_2^2 m_3}{\omega_2} + \frac{k_3 k_2 m_2}{\omega_2} + \frac{k_3 k_2 m_3}{\omega_3} \right) e^{i(k_1 x - \omega_1 t)} F_3 \bar{F}_2 \\ &\quad + N^2(k_3 - k_1) a_3 \bar{a}_1 \left(-\frac{k_3^2 m_1}{\omega_3} - \frac{k_1^2 m_3}{\omega_1} + \frac{k_3 k_1 m_1}{\omega_1} + \frac{k_3 k_1 m_3}{\omega_3} \right) e^{i(k_2 x - \omega_2 t)} F_3 \bar{F}_1 + \text{c.c.} \end{aligned}$$

Note that overbar denotes complex conjugate. There are additional terms with wavenumbers and frequencies different from that of the three waves initially assumed. These are the non-resonant terms, which are not important for resonant energy transfer, and hence are neglected.

2.1. Amplitude evolution equations for the resonant triad

From the above resonant terms of $\mathcal{O}(\epsilon^2)$, we match those terms of the LHS and the RHS that have the same frequency and horizontal wavenumber. This finally leads to

three amplitude evolution equations:

$$\frac{\partial a_1}{\partial(\epsilon_t t)} + H_1(\epsilon_n z) \frac{\partial a_1}{\partial(\epsilon_x x)} + S_1(\epsilon_n z) \frac{\partial a_1}{\partial(\epsilon_z z)} = \frac{1}{2} C_1(\epsilon_n z) a_3 \bar{a}_2 e^i \int_0^z (m_3 - m_2 - m_1) dz \quad (2.10a)$$

$$\frac{\partial a_2}{\partial(\epsilon_t t)} + H_2(\epsilon_n z) \frac{\partial a_2}{\partial(\epsilon_x x)} + S_2(\epsilon_n z) \frac{\partial a_2}{\partial(\epsilon_z z)} = \frac{1}{2} C_2(\epsilon_n z) a_3 \bar{a}_1 e^i \int_0^z (m_3 - m_1 - m_2) dz \quad (2.10b)$$

$$\frac{\partial a_3}{\partial(\epsilon_t t)} + H_3(\epsilon_n z) \frac{\partial a_3}{\partial(\epsilon_x x)} + S_3(\epsilon_n z) \frac{\partial a_3}{\partial(\epsilon_z z)} = \frac{1}{2} C_3(\epsilon_n z) a_1 a_2 e^i \int_0^z (m_1 + m_2 - m_3) dz \quad (2.10c)$$

The functions S_j , H_j , and C_j are given by:

$$S_j(\epsilon_n z) = -\frac{m_j \omega_j}{k_j^2 + m_j^2}, \quad H_n(\epsilon_z z) = \frac{k_j (N^2 - \omega_j^2)}{\omega_j (k_j^2 + m_j^2)}, \quad (2.11a)$$

$$C_1(\epsilon_n z) = \frac{N^2(k_3 - k_2)}{k_1^2 \omega_1 + m_1^2 \omega_1} \left(-\frac{k_3^2 m_2}{\omega_3} - \frac{k_2^2 m_3}{\omega_2} + \frac{k_3 k_2 m_2}{\omega_2} + \frac{k_3 k_2 m_3}{\omega_3} \right) \left(\frac{m_1}{m_2 m_3} \right)^{1/2} \\ - \frac{(\omega_3 - \omega_2)}{k_1^2 \omega_1 + m_1^2 \omega_1} \left((k_3 m_2 - k_2 m_3) (m_3^2 + k_3^2 - k_2^2 - m_2^2) \right) \left(\frac{m_1}{m_2 m_3} \right)^{1/2}, \quad (2.11b)$$

$$C_2(\epsilon_n z) = \frac{N^2(k_3 - k_1)}{k_2^2 \omega_2 + m_2^2 \omega_2} \left(-\frac{k_3^2 m_1}{\omega_3} - \frac{k_1^2 m_3}{\omega_1} + \frac{k_3 k_1 m_1}{\omega_1} + \frac{k_3 k_1 m_3}{\omega_3} \right) \left(\frac{m_2}{m_1 m_3} \right)^{1/2} \\ - \frac{(\omega_3 - \omega_1)}{k_2^2 \omega_2 + m_2^2 \omega_2} \left((k_3 m_1 - k_1 m_3) (m_3^2 + k_3^2 - k_1^2 - m_1^2) \right) \left(\frac{m_2}{m_1 m_3} \right)^{1/2}, \quad (2.11c)$$

$$C_3(\epsilon_n z) = \frac{N^2(k_1 + k_2)}{k_3^2 \omega_3 + m_3^2 \omega_3} \left(\frac{k_1^2 m_2}{\omega_1} + \frac{k_2^2 m_1}{\omega_2} - \frac{k_1 k_2 m_2}{\omega_2} - \frac{k_1 k_2 m_1}{\omega_1} \right) \left(\frac{m_3}{m_2 m_1} \right)^{1/2} \\ - \frac{(\omega_1 + \omega_2)}{k_3^2 \omega_3 + m_3^2 \omega_3} \left((k_1 m_2 - k_2 m_1) (m_2^2 + k_2^2 - k_1^2 - m_1^2) \right) \left(\frac{m_3}{m_2 m_1} \right)^{1/2}. \quad (2.11d)$$

These equations generalize the ones obtained in Lamb (2007) since in our case, the coefficients S_j , C_j and H_j are all dependent on the z -direction. The vector (H_j, S_j) denotes the (weakly varying) group speed of the j -th wave. Equations (2.10a)–(2.10c) are the amplitude evolution equations of waves, or ‘wave packets’ whose carrier waves satisfy the triad condition. The length scale of variation of the amplitude function (and also the stratification function) is chosen to be at least an order of magnitude more than the length scale (vertical wavenumber) of the waves. Hence, waves in each wave packet other than the carrier wave has negligible energy. For simplicity, we assume the initial wave amplitudes to be independent of x . Since the evolution equations are themselves not capable of creating x variations, amplitudes that are initially independent of x remains so forever (i.e. evolves only along z). The functions S_j , C_j and the exponential functions in the RHS of (2.10a)–(2.10c) influence the energy transfer, and also create amplitude variations in the z -direction, even if the waves’ amplitudes are initialized with no z -dependence. This is precisely due to the non-uniformity of the density stratification profile. In fact, the origin of these exponential functions is the non-uniformity of the density stratification profile – the vertical wavenumber does not satisfy the triad condition at all locations, which leads to mismatch in the vertical wavenumber. Thus, the argument of each exponential function represents the relative phase difference created between the waves (forming the triad) as they propagate through the non-uniformly stratified medium. Since such a mechanism

introduces wave detuning, hereafter we refer the exponential function as the *detuning function*.

The three evolution equations (2.10a)-(2.10c) are solved using RK4 method in time and second order accurate discretization scheme for the term $\partial a_j / \partial z$, where the scheme is forward or backward depending on the group speed direction of the particular wave.

2.2. Energy evaluation

The evolution of energy for these three waves is calculated by considering the kinetic energy, where kinetic energy density at an instant is given by:

$$\text{KE}_j = \frac{\rho_0}{2} (u_j^2 + w_j^2) = \frac{\rho_0}{2} \left(\left[\frac{\partial \psi_j}{\partial z} \right]^2 + \left[\frac{\partial \psi_j}{\partial x} \right]^2 \right).$$

The time averaged kinetic energy density for an internal gravity wave over its time period is given by:

$$\langle \text{KE}_j \rangle = \frac{\omega_j}{2\pi} \int_0^{2\pi/\omega_j} \frac{\rho_0}{2} \left(\left[\frac{\partial \psi_j}{\partial z} \right]^2 + \left[\frac{\partial \psi_j}{\partial x} \right]^2 \right) dt.$$

The total kinetic energy in the domain is calculated by integrating in the z -direction:

$$\text{TKE}_j = \int_0^L \langle \text{KE}_j \rangle dz = \int_0^L 2\rho_0 \left(\frac{k_j^2 + m_j^2}{m_j} \right) a_j \bar{a}_j dz, \quad (2.12)$$

where L is the length of the domain in the z -direction. We non-dimensionalize TKE_j with the initial energy of wave ‘3’: $E_j = \text{TKE}_j / \text{TKE}_3|_{t=0}$. Furthermore, we define a non-dimensional variable called the transmission coefficient, \mathfrak{T}_j , which calculates the change in the energy of each wave with respect to its initial energy. Mathematically it implies

$$\mathfrak{T}_j = \frac{E_j|_{t=t_1} - E_j|_{t=0}}{E_j|_{t=0}}, \quad (2.13)$$

where t_1 denotes the instant when the energy of the j -th wave has reached its first maxima or minima (for example, in figure 6(a), the energy of all three waves reach their first maxima or minima at $t_1 \approx 14$, which has been marked by a vertical black line). The quantity \mathfrak{T}_j can be either positive or negative depending on whether the j -th wave has gained or lost energy. The non-dimensionalised growth rate of a wave based on TKE is defined as:

$$\text{Gr}_j^E = \frac{1}{\omega_3} \frac{1}{\langle \text{TKE}_j \rangle} \frac{d(\text{TKE}_j)}{dt}. \quad (2.14)$$

3. Effect of group speed on triad interactions among infinite width waves in uniform stratification

Energy transfer between finite width internal gravity wave beams have been previously studied by Bourget *et al.* (2014) and Karimi & Akyas (2014). It was found that the width of the primary internal gravity wave is an important factor in the energy transfer; the daughter waves should spatially overlap with the primary wave for a given time so that they can exchange energy. Here, the overlap time between the different beams is mainly dependent on the group speed (apart from the individual beam width) of the internal wave beams. However, even for infinite width waves (or very large wave packets which do not move out of each other’s range), the group speed can play a role in deciding the

growth rates of the daughter waves, provided there is a spatial variation of the amplitude profile of any constituent wave (any one wave having a variation will slowly lead to all three waves having a spatially varying amplitude, as shown by Craik & Adam (1978)). Craik & Adam (1978) primarily focused on daughter waves which have the same group speed. Here we don't make any such assumptions about the group speed and study the effect of group speed on triads that are detuned. Moreover, the daughter waves which we consider have spatially (z) varying amplitude at $t = 0$. To this end, let us consider the governing equations for a triad with a constant wavenumber mismatch:

$$\frac{\partial a_1}{\partial(\epsilon_t t)} + S_1 \frac{\partial a_1}{\partial(\epsilon_z z)} = \frac{1}{2} C_1 a_3 \bar{a}_2 e^{i\Delta m z}, \quad (3.1a)$$

$$\frac{\partial a_2}{\partial(\epsilon_t t)} + S_2 \frac{\partial a_2}{\partial(\epsilon_z z)} = \frac{1}{2} C_2 a_3 \bar{a}_1 e^{i\Delta m z}, \quad (3.1b)$$

$$\frac{\partial a_3}{\partial(\epsilon_t t)} + S_3 \frac{\partial a_3}{\partial(\epsilon_z z)} = \frac{1}{2} C_3 a_1 a_2 e^{-i\Delta m z}. \quad (3.1c)$$

Here, $\Delta m = m_3 - m_1 - m_2$ is the mismatch in the vertical wavenumber, furthermore $\Delta m/m_j \sim \mathcal{O}(\epsilon_z)$ is assumed. In PSI, usually the primary wave's amplitude (here it is wave '3') is very large in comparison to the other two waves. Hence the nonlinear term in (3.1c) is negligible in the initial stages of the problem (i.e., the equation follows the scaling of A 7b). This is known as the *pump-wave approximation* (Craik & Adam 1978). Thus (3.1a)–(3.1c) reduces to:

$$\frac{\partial a_1}{\partial(\epsilon_t t)} + S_1 \frac{\partial a_1}{\partial(\epsilon_z z)} = \frac{1}{2} C_1 a_3 \bar{a}_2 e^{i\Delta m z}, \quad (3.2a)$$

$$\frac{\partial a_2}{\partial(\epsilon_t t)} + S_2 \frac{\partial a_2}{\partial(\epsilon_z z)} = \frac{1}{2} C_2 a_3 \bar{a}_1 e^{i\Delta m z}, \quad (3.2b)$$

$$\frac{\partial a_3}{\partial(\epsilon_t t)} + S_3 \frac{\partial a_3}{\partial(\epsilon_z z)} = 0. \quad (3.2c)$$

We assume an oscillatory solution for (3.2c): $a_3 = A_3 e^{i(M_3 z - S_3 M_3 t)}$, where A_3 is a constant denoting the amplitude of the wave '3' (the pump wave), and M_3 is the corresponding vertical wavenumber for the amplitude profile (plane wave solution, assumed in the previous studies, can be recovered by substituting $M_3 = 0$). This would result in two coupled equations for the daughter waves:

$$\frac{\partial a_1}{\partial(\epsilon_t t)} + S_1 \frac{\partial a_1}{\partial(\epsilon_z z)} = \frac{1}{2} C_1 A_3 e^{i(M_3 z - S_3 M_3 t)} \bar{a}_2 e^{i\Delta m z}, \quad (3.3a)$$

$$\frac{\partial a_2}{\partial(\epsilon_t t)} + S_2 \frac{\partial a_2}{\partial(\epsilon_z z)} = \frac{1}{2} C_2 A_3 e^{i(M_3 z - S_3 M_3 t)} \bar{a}_1 e^{i\Delta m z}. \quad (3.3b)$$

We assume normal mode solutions for a_1 and a_2 : $a_1 = \tilde{a}_1(\epsilon_t t) e^{i(M_1 z - M_1 S_1 t)}$ and $a_2 = \tilde{a}_2(\epsilon_t t) e^{i(M_2 z - M_2 S_2 t)}$, where M_1 and M_2 are respectively the vertical wavenumbers of the amplitude profiles of wave '1' and wave '2'. The relation between M_1 , M_2 , M_3 , and Δm is then given by: $M_2 = M_3 + \Delta m - M_1$, which makes the problem variable separable. Substituting these in (3.3a)–(3.3b) reduces the governing equations to:

$$\frac{\partial \tilde{a}_1}{\partial(\epsilon_t t)} + i(M_1 S_1 - M_3 S_3) \tilde{a}_1 = \frac{1}{2} C_1 A_3 \bar{\tilde{a}}_2, \quad (3.4a)$$

$$\frac{\partial \tilde{a}_2}{\partial(\epsilon_t t)} + i(M_3 + \Delta m - M_1) S_2 \tilde{a}_2 = \frac{1}{2} C_2 A_3 \bar{\tilde{a}}_1. \quad (3.4b)$$

If we consider the solution of \tilde{a}_j (where $j = 1, 2$) to be of the form: $\tilde{a}_j = e^{-i\Omega_j t}$, then the growth rate of the \tilde{a}_j is defined as: $\text{GR}_j = \Im(\Omega_j)$ (note they are different from Gr_j^E in (2.14)). The amplitude growth rates then turn out to be:

$$\text{GR}_1 = \text{GR}_2 = \sqrt{C_1 C_2 A_3^2 - \{M_1 S_1 - M_3 S_3 + (M_3 + \Delta m - M_1) S_2\}^2}. \quad (3.5)$$

For maximum amplitude growth rates, we have

$$M_1 S_1 - M_3 S_3 + (M_3 + \Delta m - M_1) S_2 = 0. \quad (3.6)$$

For details regarding this derivation, see appendix B. This is the most general condition for obtaining maximum growth rates since it allows all three waves in the triad to have a spatial variation as well as a wavenumber mismatch. We note here that special cases of the condition we derived have been explored previously. For example, Craik & Adam (1978) studied the parameter space where $S_1 = S_2$ when $M_3 = 0$, in which case a detuned triad cannot have the same growth rate as a non-detuned triad; as the detuning is increased, the growth rate keeps on decreasing for any normal mode form of a_1 and a_2 . In addition, McEwan & Plumb (1977) explored the parameter space when $S_1 \neq S_2$ when $M_3 = 0$.

In detuned triads, the primary wave need not degrade to small amplitude daughter waves even if the growth rates predicted by the normal mode forms are positive. This is shown by an example below. The governing equations considered are (3.1a)–(3.1c). We assume normal mode forms for the amplitudes: $a_1 = \tilde{a}_1(\epsilon_t t) e^{iM_1 z}$, $a_2 = \tilde{a}_2(\epsilon_t t) e^{iM_2 z}$ and $a_3 = \tilde{a}_3(\epsilon_t t) e^{iM_3 z}$. It is also assumed that $M_1 = \Delta m$, $M_2 = 0$ and $M_3 = 0$, which reduces the governing equations to a purely temporal form given by:

$$\frac{\partial \tilde{a}_1}{\partial(\epsilon_t t)} + i\Delta m S_1 \tilde{a}_1 = \frac{1}{2} C_1 \tilde{a}_3 \bar{\tilde{a}}_2, \quad (3.7a)$$

$$\frac{\partial \tilde{a}_2}{\partial(\epsilon_t t)} = \frac{1}{2} C_2 \tilde{a}_3 \bar{\tilde{a}}_1, \quad (3.7b)$$

$$\frac{\partial \tilde{a}_3}{\partial(\epsilon_t t)} = \frac{1}{2} C_3 \tilde{a}_1 \tilde{a}_2. \quad (3.7c)$$

The above set of equations are also similar to the equations given in Craik (1988) for the triad interaction between waves which have a frequency mismatch between them. Here (3.7a)–(3.7c) are solved numerically and the results are given in figure 1. The non-linear coupling coefficients are as follows: $C_1 = -8.6 \times 10^{-4} \text{m}^{-3/2}$, $C_2 = -8.56 \times 10^{-4} \text{m}^{-3/2}$, $C_3 = 3.2 \times 10^{-3} \text{m}^{-3/2}$ and $S_1 = 3.4 \times 10^{-3} \text{ms}^{-1}$, which are the same as the triads used in §3.1. We consider two separate cases with $\tilde{a}_1(0) = \tilde{a}_2(0) = 1 \times 10^{-6} \text{m}^{3/2} \text{s}^{-1}$, while the other initial conditions are different, and are as follows:

(i) Detuned Case: $\Delta m = 2.4 \times 10^{-3} \text{m}^{-1}$ (which results in $\Delta m/m_3 = 0.12$) and $\tilde{a}_3(0) = 1 \times 10^{-2} \text{m}^{3/2} \text{s}^{-1}$. Furthermore, $(\Delta m S_1)^2 / (C_1 C_2 A_3^2) \approx 0.91$. Using (3.5), the normal mode growth rate of a_1 is found to be $\text{GR}_1 = 2.58 \times 10^{-6} \text{s}^{-1}$.

(ii) Non-detuned Case: $\Delta m = 0$ and $\tilde{a}_3(0) = 1 \times 10^{-3} \text{m}^{3/2} \text{s}^{-1}$. The normal mode growth rate of a_1 is $\text{GR}_1 = 8.6 \times 10^{-7} \text{s}^{-1}$.

Figure 1(a) shows that the primary wave in the ‘Detuned Case’ was able to exchange only 9% of its total energy, while figure 1(b) shows that the primary wave in the ‘Non-detuned Case’ was able to exchange all of its energy, despite the fact that the normal mode growth rate is higher for the ‘Detuned Case’. This occurs for a detuned triad in the parameter regime $\{M_1 S_1 - M_3 S_3 + (M_3 + \Delta m - M_1) S_2\}^2 / (C_1 C_2 A_3^2) \approx 1$. Hence the normal mode forms in the pump-wave approximation predict accurate growth rates *only* during the initial stages of the problem, but fails to provide the complete picture of energy exchange in the case of a detuned triad. Furthermore, this implies that even when the normal mode

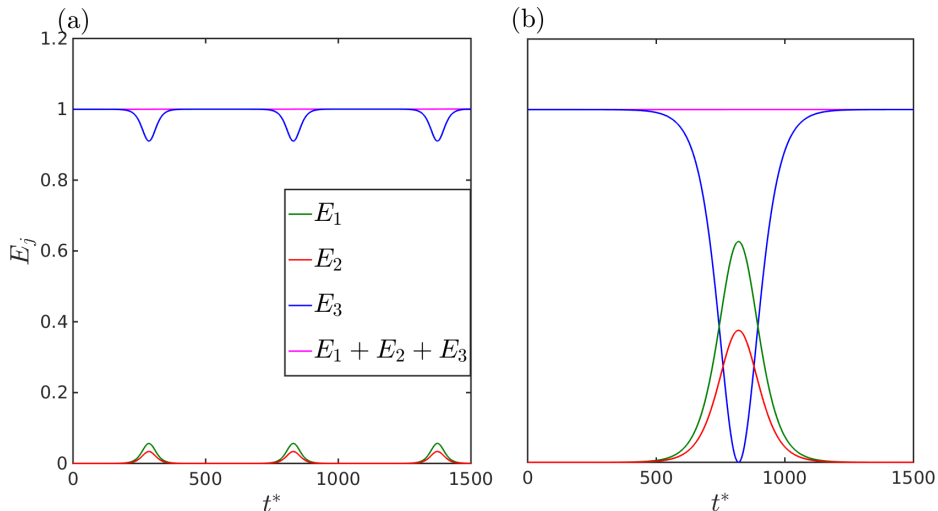


Figure 1: Comparison of time evolution of energy for waves which are detuned and non-detuned. The abscissa $t^* = t\omega_3/2\pi$ represents non-dimensional time. (a) The detuned case. Here the pump wave amplitude at $t = 0$ is $\tilde{a}_3(0) = 1 \times 10^{-2} \text{m}^{3/2} \text{s}^{-1}$. (b) The non-detuned case. The pump wave amplitude at $t = 0$ is $\tilde{a}_3(0) = 1 \times 10^{-3} \text{m}^{3/2} \text{s}^{-1}$, and is therefore a decade smaller than (a).

growth rates are nearly the same, the amount of energy exchanged can be quite different between a non-detuned triad and a detuned triad.

3.1. Interaction between detuned wavepackets in uniform stratification

In this sub-section, we focus on energy transfer between resonant as well as near-resonant (wavenumber mismatch) wave packets in uniform stratification. As mentioned earlier, energy transfer between finite width internal gravity wave beams have been previously studied by Karimi & Akylas (2014) and Bourget *et al.* (2014). Furthermore, near-resonant (frequency mismatch) wave packets were studied by Huang *et al.* (2007), who found that increasing the width of the wave packets do not generally change the degree of interaction, however below our findings show significant change in the amount of energy transfer with variations in the wave packet width.

In §3 it was shown that in general, as the detuning is increased, the growth rate and energy transfer between the waves decreased (see (3.5)); this is true even for infinite width waves. For a finite wave packet, it can therefore be expected that detuning will add an additional constraint on the size or the amplitude of the wave packets; that is, the packets' size will have to be larger in comparison to a non-detuned case for the wave packet to get degraded, that is, lose the same percentage of energy through PSI.

For studying the energy transfer between detuned wave packets, a triad is chosen (i.e., group speed and nonlinear coefficients are fixed). The size of the wave packets constituting the triad are varied. Moreover, for each wave packet size, the detuning between the waves is slowly varied and the effect of this detuning on the energy transferred to the daughter wave packets is studied. McEwan & Plumb (1977) explored the parameter space where the pump wave was of infinite width while the daughter waves had a finite size. In our case, the pump wave also has a finite width (hence a pump wave packet), and the size of the primary wave packet is varied. We consider vertically confined wave packets; such

packets have also been recently studied by van den Bremer *et al.* (2019), albeit for a different purpose. Another important point is that in a realistic system, the variation in background stratification is needed to cause a detuning of vertical wavenumber, but here we simply keep the background stratification and all other parameters constant (except the detuning in vertical wavenumber which we vary independently) so that the nonlinear coefficients and group speed are all held constant, and the effect of detuning can be strictly focused. The governing equations (3.1a)–(3.1c) are solved. The initial amplitude profile for all the three waves forming the triad are the same, and is chosen as Gaussian shape in the z -direction:

$$a_1 = a_2 = 10^{-5} \times e^{-((z-z_c)/S_a)^2} \quad a_3 = 10^{-2} \times e^{-((z-z_c)/S_a)^2},$$

where z_c is simply a reference point in the domain. The same profiles are used in all simulations in this section. We see that wave 3's energy is much more than the other two waves. The system is initialized in such a way to study the evolution of energy of the two lesser energy wave packets, similar to PSI. The above amplitude profiles indicate all the wave packets overlap at $t = 0$. The size of the wavepackets is varied through the parameter S_a . The following frequencies and wavenumbers are chosen: $\omega_1 = 1.04 \times 10^{-4} \text{s}^{-1}$, $\omega_2 = 1.77 \times 10^{-4} \text{s}^{-1}$, $\omega_3 = 2.81 \times 10^{-4} \text{s}^{-1}$, and $k_1 = 0.0031 \text{m}^{-1}$, $k_2 = -0.009 \text{m}^{-1}$, $k_3 = 0.0059 \text{m}^{-1}$. The stratification is fixed at $N = 0.001 \text{s}^{-1}$. The governing equations (3.1a)–(3.1c) are solved and Δm is varied. The quantity Δm is non-dimensionalized with the primary wave's vertical wavelength (λ_3). The variation of Δm is such that $\Delta m/m_3 = 0$ to $\Delta m/m_3 = 0.1$ for all different wave packet sizes used. The wave packet sizes chosen for this analysis are $S_a = 30\lambda_3, 60\lambda_3, 120\lambda_3$ and $240\lambda_3$. For $S_a = 30\lambda_3$, the primary wave packet exchanged (for all the values of Δm) only about 1% of its total energy at best. The variation in energy transferred from the primary wave packet to the daughter wave packets, with increase in Δm is shown in figure 2 for wave packet size of $S_a = 60\lambda_3$ and $S_a = 240\lambda_3$. For a wave packet size of $S_a = 120\lambda_3$, for all values of Δm , the primary wave packet had transferred more (less) energy than $S_a = 60\lambda_3$ ($S_a = 240\lambda_3$). It shows that as the detuning $\Delta m/m_3$ is increased, the energy transfer is severely affected, that is, the amount of energy transferred by the primary wave packet to the daughter wave packets become lesser. For example, when $S_a = 60\lambda_3$, the primary wave packet in the non-detuned case transferred 30% of its total energy, while the transfer was less than 1% for $\Delta m/m_3 = 0.1$. This happens regardless of the size of the wave packets with which the system is initialized. Interestingly we can see that for the wave packet size of $S_a = 240\lambda_3$, the case of $\Delta m/m_3 = 0.04$ has exchanged more energy than the non-detuned wave packet at a certain point of time. That is, $S_a = 240\lambda_3$ ($\Delta m = 0$) transferred 56% of its total energy at $t^* = 84$, however it transferred 66% of its total energy at $t^* = 106$ when $\Delta m/m_3 = 0.04$; compare figures 2(a) and 2(c).

This is because in the case of no detuning, the wave packets exchange energy faster than the detuned packets. The energy transfer near the top region of the Gaussian shape (in comparison to the flank regions of the Gaussian bump) of the primary wave packet is so fast that at $t^* \approx 40$, the direction of energy transfer in that particular region reverses, that is, the primary wave starts gaining energy near the 'top' of the Gaussian region. Meanwhile the flank regions of the primary wave packet still provides energy to the daughter waves. Hence the net growth rate (2.14) of the daughter wave packets becomes near zero (near $t^* = 40$); see figure 2(a). As t^* further increases, the daughter waves provide more energy to the primary waves than it takes away, therefore the net energy of the primary wave packet increases. The time for reversal of energy transfer (daughter wave packets providing energy to the primary wave packet) is smaller for a

non-detuned case than the detuned cases. Meanwhile for a detuned case, the reversal of energy transfer near the top region of the Gaussian ‘mountain’ is slower which results in outer regions of the Gaussian mountain transferring more energy (before the reversal of energy transfer) in comparison to the non-detuned packet. To see this in more detail, at $t^* = 53$, the primary wave has transferred around 80% of its energy to the daughter waves ($E_3 = 0.2$), if we exclude the energy which was returned back from the daughter waves. At the same t^* for $\Delta m/m_3 = 0.04$ (figure 2(c)), the primary wave has transferred around 71% of its energy to the daughter waves ($E_3 = 0.29$) excluding the energy transferred back from the daughter waves. Hence the primary reason a detuned packet seems to transfer more energy than the non-detuned packet is because the latter has a reversal of energy transfer near the top of the Gaussian ‘mountain’.

It was observed that as the size of the wave packets is increased, the energy transferred to the daughter wave packets in the case of no detuning increases monotonically, which is expected from the results of Karimi & Akylas (2014) or Bourget *et al.* (2014). It was also observed that for $\Delta m/m_3 = 0.1$, increasing the size beyond $S_a = 240\lambda_3$ did not result in increased energy transfer to daughter wave packets. For example, the case of $S_a = 960\lambda_3$ with $\Delta m/m_3 = 0.1$ lost approximately 20% (at $t^* \approx 130$) of its total energy, which is similar to the case of $S_a = 240\lambda_3$. Observe that this saturation of energy transfer (as the detuning is increased) is consistent with the result shown in §3, where even for positive growth rates, the primary wave did not transfer more than 9% of its total energy.

To summarize, energy transfer in finite wave packets is monotonically affected as the detuning increases, the amount of energy transferred from the primary to the daughter wave packets become lesser. For very high detuning, the energy transferred to the daughter waves are considerably lesser in comparison to the non-detuned wave packets. It can also be noticed that the wave packet size has to be larger for a detuned wave packet than a non-detuned wave packet in order to exchange the same percentage of energy. For high levels of detuning, increasing the wave packet size (of all three waves) did not result in more energy being transferred from the primary wave packet.

3.2. Wavepackets interacting in weakly varying stratifications

In this subsection we focus on wave packets exchanging energy in weakly varying stratification. Energy transfer of finite width wave packets in weakly non-uniform stratification is mainly affected by three factors:

- (i) Varying stratification, which causes wave detuning.
- (ii) Nonlinear coupling coefficients (C_i), which are directly proportional (effectively) to the square root of the local stratification value.
- (iii) Varying group speed of the wave packets, resulting from varying stratification (as shown earlier, group speed is key in deciding the effect of detuning between the waves).

When waves travel from the base stratification where the triad conditions are perfectly met, to a higher stratification and assuming their angular frequency and horizontal wavenumbers stay constant, the vertical group speeds decrease while the non-linear coupling coefficients increase. Since reduction of group speed increases the interaction time between the wave packets, and increase in the non-linear coupling coefficients increase the growth rates, we can expect that wave packets of a given size (moving from a lower to a higher stratification) can transfer more energy among themselves in the higher stratification than in the base stratification where the triad conditions are perfectly met, provided the effect of mismatch in the vertical wavenumbers is less. This can be explained using the example below.

The governing equations considered here are (2.10a)–(2.10c) with x independent am-

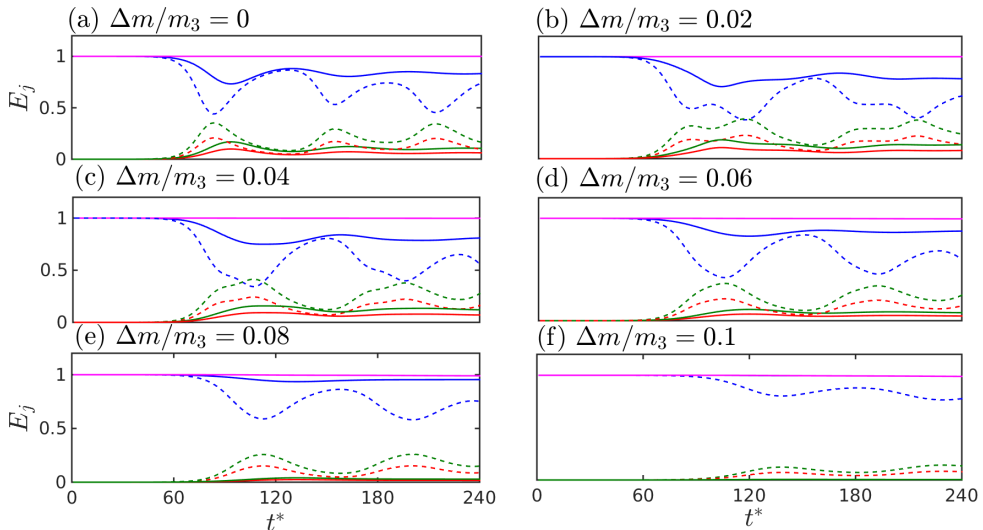


Figure 2: Energy evolution plots for (a) $\Delta m/m_3 = 0.00$ (non-detuned), (b) $\Delta m/m_3 = 0.02$, (c) $\Delta m/m_3 = 0.04$, (d) $\Delta m/m_3 = 0.06$, (e) $\Delta m/m_3 = 0.08$, and (f) $\Delta m/m_3 = 0.1$. Two different wavepacket sizes are considered: $S_a = 60\lambda_3$ (continuous curves) and $S_a = 240\lambda_3$ (dashed curves). Green curves signify E_1 , red curves signify E_2 , blue curves signify E_3 and magenta curves signify total energy $E_1 + E_2 + E_3$.

plitudes:

$$\frac{\partial a_1}{\partial(\epsilon t)} + S_1 \frac{\partial a_1}{\partial(\epsilon_z z)} = \frac{1}{2} C_1 a_3 \bar{a}_2 e^{i \int_0^z -(m_1+m_2-m_3) dz}, \quad (3.8a)$$

$$\frac{\partial a_2}{\partial(\epsilon t)} + S_2 \frac{\partial a_2}{\partial(\epsilon_z z)} = \frac{1}{2} C_2 a_3 \bar{a}_1 e^{i \int_0^z -(m_1+m_2-m_3) dz}, \quad (3.8b)$$

$$\frac{\partial a_3}{\partial(\epsilon t)} + S_3 \frac{\partial a_3}{\partial(\epsilon_z z)} = \frac{1}{2} C_3 a_1 a_2 e^{i \int_0^z (m_1+m_2-m_3) dz}. \quad (3.8c)$$

Like §3.1, the initial amplitude profile for all the three wave packets forming a triad are assumed to be Gaussian in the z -direction:

$$a_1 = a_2 = 10^{-5} \times e^{-((z-z_c)/S_a)^2} \quad \text{and} \quad a_3 = 10^{-2} \times e^{-((z-z_c)/S_a)^2},$$

where $S_a = 60\lambda_3$ and λ_3 is the vertical wavelength of ‘wave 3’ in the uniformly stratified region. The magnitude of the amplitude function (of the primary wave, or the wave which has the most energy) is chosen such that its velocity is $\sim 10^{-3}\text{ms}^{-1} - 10^{-4}\text{ms}^{-1}$. These values have been used as the magnitude of the base flow in Lamb (2004) or Echeverri & Peacock (2010). Initially, waves 1 and 2 have much smaller energy than wave 3 since our intention is to simulate a PSI, i.e. a situation where a wave with large energy loses energy to small noise. The angular frequencies of the constituent waves of the triad are $\omega_1 = 1.04 \times 10^{-4}\text{s}^{-1}$, $\omega_2 = 1.77 \times 10^{-4}\text{s}^{-1}$, and $\omega_3 = 2.81 \times 10^{-4}\text{s}^{-1}$, while the horizontal wavenumbers are $k_1 = 0.0031\text{m}^{-1}$, $k_2 = -0.009\text{m}^{-1}$, and $k_3 = 0.0059\text{m}^{-1}$. They obey the triad condition $(k_1, \omega_1) + (k_2, \omega_2) = (k_3, \omega_3)$. For weakly varying stratification, we consider a Gaussian distribution for the buoyancy frequency given by:

$$N(\epsilon_n z) = N_b + N_v e^{-((z-z_c)/S_g)^2}, \quad (3.9)$$

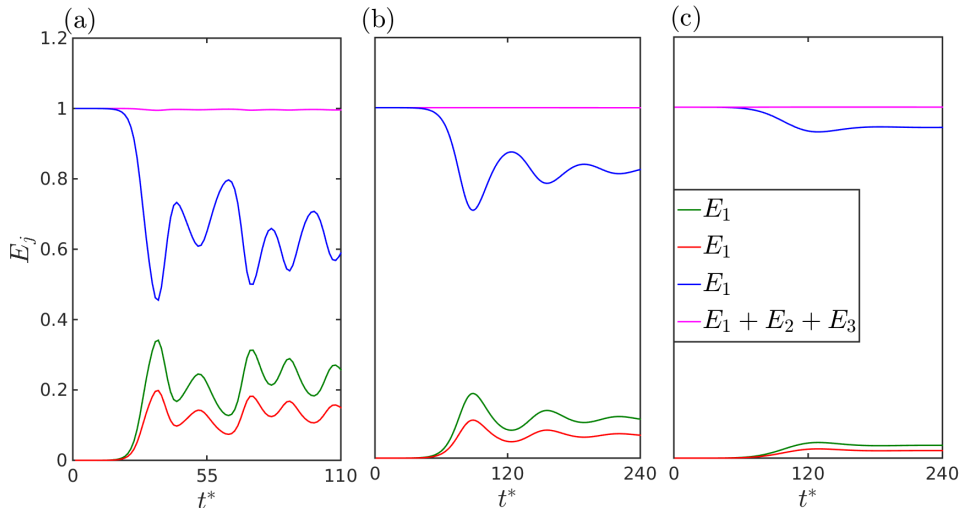


Figure 3: Comparison of time evolution of energy for wave packet triads in uniform and weakly varying stratifications. (a) When waves move to a region of higher stratification from a base stratification where triad conditions are perfectly met, $\sim 55\%$ of the energy of the primary wave (blue curve) is transferred to the daughter waves. (b) In a uniform stratification case, the primary wave has transferred $\sim 30\%$ of its total energy to the daughter waves. (c) When waves move to a region of lower stratification from a base stratification where triad conditions are perfectly met, only $\sim 8\%$ of the energy of the primary wave is transferred to the daughter waves. The time scale of energy transfer increases from (a)–(c).

where $N_b = 10^{-3}\text{s}^{-1}$. Now we compare the energy transfer between the wave packets in a uniform stratification ($N_v = 0$) and a stratification profile where $N_v = 9N_b$ and $S_g = 40S_a$. While in the first case ($N_v = 0$), the triad condition is assumed to be always satisfied, in the second case it is satisfied in the region where $N = N_b$ (i.e. far from the Gaussian bump). Mathematically, we have

$$k_3\sqrt{N_b^2/\omega_3^2 - 1} - k_2\sqrt{N_b^2/\omega_2^2 - 1} + k_1\sqrt{N_b^2/\omega_1^2 - 1} = 0.$$

When waves of given horizontal wavenumbers and angular frequencies travel through a variable stratification, the vertical wavenumbers change accordingly. For this particular triad, the stratification profile (3.9) produces $\Delta m/m_3 = 0.09$, where Δm is the maximum detuning in vertical wavenumber, and is given by:

$$\Delta m = k_2\sqrt{(N_b + N_v)^2/\omega_2^2 - 1} + k_1\sqrt{(N_b + N_v)^2/\omega_1^2 - 1} - k_3\sqrt{(N_b + N_v)^2/\omega_3^2 - 1}.$$

This occurs at the ‘top’ ($z = z_c$) of the ‘Gaussian mountain’ of the buoyancy frequency. Meanwhile, the group speed of the waves (given by $S_j = -\omega_j m_j / (m_j^2 + k_j^2)$) decreases approximately 9 times due to the increase in stratification near the top of the Gaussian mountain, since the vertical wavenumber is directly proportional to the local stratification value when the waves’ angular frequency is such that $N^2/\omega^2 \gg 1$. The nonlinear coupling coefficients (C_j) are also proportional to the square root of the local stratification value. Hence in effect, the nonlinear terms get much more strengthened (near the top of the buoyancy frequency Gaussian mountain) in comparison to the group speed term, leading

to an enhanced energy transfer and higher growth rate of the daughter waves. This phenomena is shown in figure 3; energy transfer in the high buoyancy frequency region is higher in comparison to that in the uniformly stratified region (where the triad conditions are perfectly met), compare figures 3(a) and 3(b). We note in passing that $\Delta m/m_3 = 0.09$ with the same set of triad resulted in a decreased energy transfer §3.1. Hence in summary, the growth rates of the daughter waves *always* increase and when they move to a region of higher stratification from a base stratification where the triad condition is satisfied; provided, angular frequencies of the waves are such that $N^2/\omega^2 \gg 1$. In oceanic conditions, a wave packet created near the bottom topography is more susceptible to PSI near the pycnocline region, since in oceans, waves generally created via semi-diurnal tides mostly have $N^2/\omega_{sd}^2 \gg 1$, where ω_{sd} is the semi-diurnal frequency.

In situations where waves move from a base stratification where the triad condition is satisfied to a region of lower stratification (i.e., $N_v < 0$ in (3.9)), in addition to wave detuning, this results in increased group speed and reduced nonlinear coupling coefficients, hence the growth rate of the daughter wave packets will always be lesser. This is shown in figure 3(c); here the stratification profile (3.9) has the same N_b as in the previous cases, however $N_v = -0.55N_b$ and $S_g = S_a$. All other parameters as well as the initial conditions are the same as the simulation shown in figure 3(a). We note here that this particular case is not only applicable for $N^2/\omega^2 \gg 1$, it is also valid for $N^2/\omega^2 \approx 1$.

For triads with wave packets satisfying $N^2/\omega^2 \approx 1$, even a small increase in stratification results in a high detuning of vertical wavenumbers. However, a small change in stratification has nearly no effect on the group speeds and nonlinear coupling coefficients. Such systems behave very similar to those considered in §3.1; where the mismatch in vertical wavenumbers ($\Delta m/m_3$) was increased independently without altering the vertical group speed of the waves or the non-linear coupling coefficients. This is purely a consequence of the dispersion relation of internal gravity waves. This is shown numerically by considering a different triad. The energy transfer is compared between two different stratifications, where one is the uniform base stratification where the triad conditions are met, and the other stratification is also uniform but slightly higher than the base stratification which causes a detuning in vertical wavenumber.

In this numerical experiment, we choose the frequencies of the constituent waves to be respectively $\omega_1 = 9.9 \times 10^{-4}\text{s}^{-1}$, $\omega_2 = 2.1 \times 10^{-3}\text{s}^{-1}$, and $\omega_3 = 3.1 \times 10^{-4}\text{s}^{-1}$, while the respective horizontal wavenumbers are $k_1 = 0.0128\text{m}^{-1}$, $k_2 = -0.0500\text{m}^{-1}$, and $k_3 = -0.0372\text{m}^{-1}$. The initial amplitudes profiles for both stratifications are:

$$a_1 = a_2 = 10^{-5} \times e^{-((z-z_c)/S_a)^2} \quad \text{and} \quad a_3 = 10^{-2} \times e^{-((z-z_c)/S_a)^2},$$

where $S_a = 120\lambda_3$. The base stratification is $N_b = 4 \times 10^{-3}\text{s}^{-1}$ and the stratification which introduces detuning is given by $N_b = 1.4 \times N_b$, yielding $\omega_3/N_b = 0.77$. Figure 4(a) shows the energy evolution of the wave packets in the base stratification and figure 4(b) shows the same for the stratification which causes detuning. Figures 4(c) and 4(d) respectively show Gr_1^E for the base stratification and the stratification which causes detuning. The rate of energy transfer for the case in figure 4(a) is more than that in figure 4(b), even though the stratification is slightly higher in the case of figure 4(b). In fact, $\max(\text{Gr}_1^E)$ in figure 4(c) is 59% higher than $\max(\text{Gr}_1^E)$ in that of figure 4(d). Here the energy transfer is mainly effected by detuning (of vertical wavenumbers) due to the increased stratification.

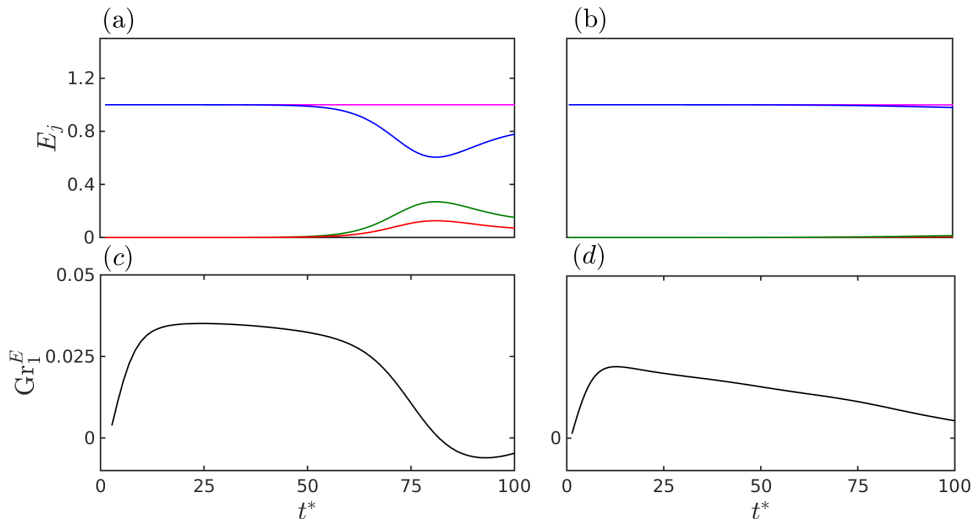


Figure 4: Comparison of energy evolution plots for wave packets in (a) uniform base stratification where the triad condition is perfectly met, and (b) slightly higher uniform stratification where the triad conditions are not met. Green, red and blue curves respectively signify E_1 , E_2 , and E_3 , and magenta curves represent total energy $E_1 + E_2 + E_3$. (c) Evolution of Gr_1^E corresponding to (a), and (d) the same corresponding to (b).

4. Effect of localized variable stratification on energy transfer between three waves packets with same order of energy

In this section, we focus on the effect of variable stratification, which is localized in space, on the energy transfer between three wave packets of size much larger in comparison to the region where stratification varies. Using the definitions as §3.2, this would mean: $S_a/S_g \gg 1$, where the S_a and S_g are the standard deviations of the Gaussian profile used for the amplitude function (a_i) of the waves and the background buoyancy frequency respectively. We consider cases where all three wave packets have the same order of magnitude of energy. In such cases, even though the stratification varies in a small region in comparison to the wave packets' size, the effect of this variable stratification on the energy transfer between the packets can still be considerable. We again consider the governing equations (3.8a)–(3.8c). We consider three separate cases where the initial amplitude profile for all the three wave packets forming the triad are the same, and is chosen to be a Gaussian distribution in z -direction:

$$a_1 = a_2 = a_3 = 10^{-2} \times e^{-((z-z_c)/S_a)^2},$$

where $S_a = 400\lambda_3$. The amplitude profile is shown in figure 5(a). This results in wave packets of width much larger than that of the stratification profiles considered below (Cases 1–3); see figure 5(b). The frequencies of the constituent waves are respectively $\omega_1 = 1.04 \times 10^{-4} \text{s}^{-1}$, $\omega_2 = 1.77 \times 10^{-4} \text{s}^{-1}$, and $\omega_3 = 2.81 \times 10^{-4} \text{s}^{-1}$, while the respective horizontal wavenumbers are $k_1 = 0.0031 \text{m}^{-1}$, $k_2 = -0.0090 \text{m}^{-1}$, and $k_3 = -0.0059 \text{m}^{-1}$. They obey the triad condition $(k_1, \omega_1) + (k_2, \omega_2) = (k_3, \omega_3)$. The initial amplitude profiles and the constituent triad waves are same in all three cases. The buoyancy frequency

profile is given according to the following Gaussian distribution:

$$N(\epsilon_n z) = N_b + N_v e^{-((z-z_c)/S_g)^2},$$

where $N_b = 10^{-3} \text{s}^{-1}$ and z_c is chosen to be the mid-point of the domain. Now we consider 3 stratification profiles which are given below:

- (i) Case 1 – Uniform stratification: $N_v = 0$.
- (ii) Case 2 – Pycnocline with parameters: $N_v = 1.68N_b$, $S_g = 20\lambda_3$.
- (iii) Case 3 – Pycnocline with parameters: $N_v = 1.68N_b$, $S_g = 40\lambda_3$.

The second and the third stratification profiles are chosen such that they respectively introduce a shift of $\pi/2$ and π in the relative phase difference of the waves' amplitude (when the waves pass through the nonlinear stratification). Hence the detuning function looks like a step function as shown in figure 5(c). The energy exchange figures for the three different stratification profiles are shown in figure 6. It can be seen that the energy evolution plots are different in the three cases shown. For example, the transmission coefficients for Case 1 are $\mathfrak{T}_1 = -0.99$, $\mathfrak{T}_2 = -0.99$ and $\mathfrak{T}_3 = 3.7$, while the transmission coefficients for Case 2 are $\mathfrak{T}_1 = -0.6$, $\mathfrak{T}_2 = -0.67$ and $\mathfrak{T}_3 = 2.29$. This means that wave packets '2' and '3' were able to exchange 99% of their initial energy in Case 1. Meanwhile in Case 2, wave packets '2' and '3' respectively exchanged only 67% and 60% of their initial energies. The energy transfer is different between uniform and the two different non-uniform stratification cases (Cases 2 and 3) because of the detuning function, which changes the relative phase difference between the waves as the waves move through the region where the buoyancy frequency is nonlinear. The fact that the phase difference between the waves play a key role in the energy transfer process was reported by Bustamante & Kartashova (2009). Below we show the effect of phase difference by simplifying the governing equations.

The governing equations for Case 2 for very large distances from the non-linearly stratified region will approximately behave without any z -dependence in the initial stages of problem (for very large width wave packets this is reasonably good approximation). Hence the governing equations (3.8a)–(3.8c) can be simplified to:

$$z \rightarrow -\infty \quad \frac{\partial a_1}{\partial(\epsilon_t t)} = \frac{1}{2} C_1 a_3 \bar{a}_2 \quad z \rightarrow \infty \quad \frac{\partial a_1}{\partial(\epsilon_t t)} = \frac{1}{2} C_1 a_3 \bar{a}_2 e^{i\pi/2} \quad (4.1a)$$

$$\frac{\partial a_2}{\partial(\epsilon_t t)} = \frac{1}{2} C_2 a_3 \bar{a}_1 \quad \frac{\partial a_2}{\partial(\epsilon_t t)} = \frac{1}{2} C_1 a_3 \bar{a}_1 e^{i\pi/2} \quad (4.1b)$$

$$\frac{\partial a_3}{\partial(\epsilon_t t)} = \frac{1}{2} C_3 a_1 a_2 \quad \frac{\partial a_3}{\partial(\epsilon_t t)} = \frac{1}{2} C_3 a_1 a_2 e^{-i\pi/2} \quad (4.1c)$$

Now we assume that $a_j = |a_j| \times \text{ph}(a_j)$ (Craik 1988), where $\text{ph}(\cdot)$ denotes the phase, the governing equations can be reduced to (after some algebraic steps):

$$z \rightarrow -\infty \quad \frac{\partial |a_1|}{\partial(\epsilon_t t)} = \frac{1}{2} C_1 |a_2| |a_3| \cos(\eta), \quad (4.2a)$$

$$\frac{\partial |a_2|}{\partial(\epsilon_t t)} = \frac{1}{2} C_2 |a_1| |a_3| \cos(\eta), \quad (4.2b)$$

$$\frac{\partial |a_3|}{\partial(\epsilon_t t)} = \frac{1}{2} C_3 |a_2| |a_1| \cos(\eta), \quad (4.2c)$$

$$\frac{\partial \eta}{\partial(\epsilon_t t)} = -\frac{1}{2} |a_1| |a_2| |a_3| \left(\frac{C_3}{|a_3|^2} + \frac{C_2}{|a_2|^2} + \frac{C_1}{|a_1|^2} \right) \sin(\eta), \quad (4.2d)$$

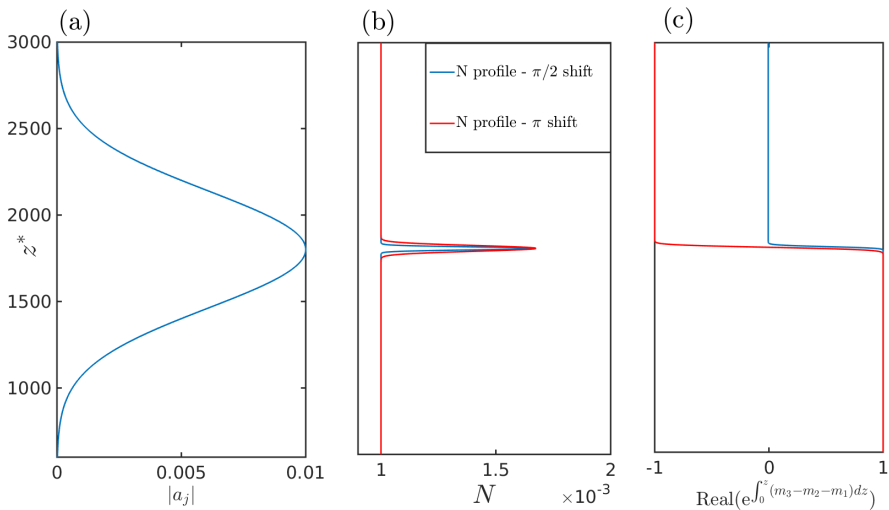


Figure 5: (a) Amplitude profile for all three waves for all the cases. (b) The stratification profiles used for Case '2' and Case '3'. (c) The detuning functions of Case '2' and Case '3'. Detuning function has a step-function like structure which makes the energy transfer before and after the step different.

$$z \rightarrow \infty \quad \frac{\partial |a_1|}{\partial(\epsilon_i t)} = \frac{1}{2} C_1 |a_2| |a_3| \cos(\eta_1), \quad (4.3a)$$

$$\frac{\partial |a_2|}{\partial(\epsilon_i t)} = \frac{1}{2} C_2 |a_1| |a_3| \cos(\eta_1), \quad (4.3b)$$

$$\frac{\partial |a_3|}{\partial(\epsilon_i t)} = \frac{1}{2} C_3 |a_2| |a_1| \cos(\eta_1), \quad (4.3c)$$

$$\frac{\partial \eta_1}{\partial(\epsilon_i t)} = -\frac{1}{2} |a_1| |a_2| |a_3| \left(\frac{C_3}{|a_3|^2} + \frac{C_2}{|a_2|^2} + \frac{C_1}{|a_1|^2} \right) \sin(\eta_1) \quad (4.3d)$$

where $\eta = \text{ph}(a_1) + \text{ph}(a_2) - \text{ph}(a_3)$ and $\eta_1 = \eta - \pi/2$.

The absolute value of the amplitudes of all three waves as $z \rightarrow -\infty$ and $z \rightarrow \infty$ are same at $t = 0$ because the wave packets are symmetric around z_c at $t = 0$. The difference between the two regions comes from the phase difference η and η_1 . The phase differences η and η_1 are such that $\eta = 0$ at $t = 0$ for $z \rightarrow -\infty$ while $\eta_1 = -\pi/2$ at $t = 0$ for $z \rightarrow \infty$. This difference between the two regions caused by the detuning function makes the energy transfer different from a uniform stratification, where there is no spatial variation (hence both regions, $z \rightarrow \infty$ and $z \rightarrow -\infty$ behaves the same way). A simple procedure to identify whether the phase shift introduced by the detuning function will affect the energy transfer between the waves is as follows. Let us assume that the phase difference between the waves is $\eta = \eta_i$ (as $z \rightarrow -\infty$). After the wave packets pass through the nonlinear stratification region, the phase difference will be $\eta_1 = \eta_i + \eta_d$ (as $z \rightarrow \infty$), where η_d is the phase difference caused by the nonlinear stratification. The only condition that would make the governing equations evolve the same way, both before ($z \rightarrow -\infty$) and after ($z \rightarrow \infty$) the waves pass through the non-linear stratification, is $\cos(\eta_i) = \cos(\eta_i + \eta_d)$ and $\sin(\eta_i) = \sin(\eta_i + \eta_d)$. This is the only way the set of governing equations (4.2a)–(4.2d) and (4.3a)–(4.3d) would evolve in time similarly. Case 2 was done

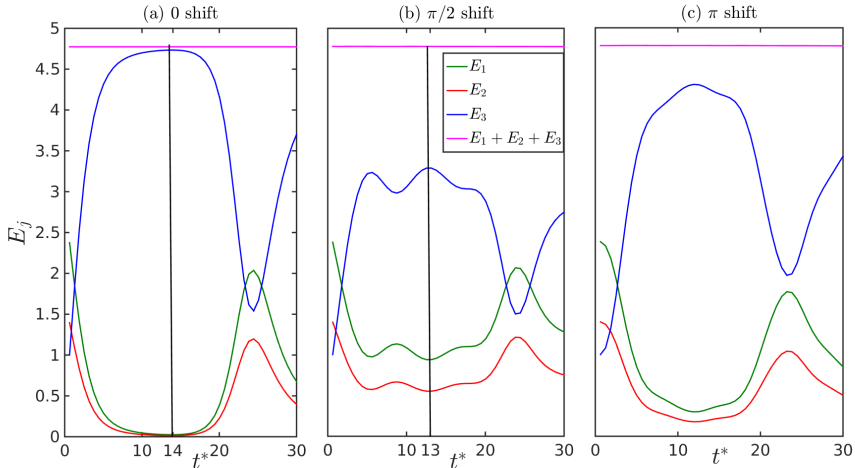


Figure 6: Energy evolution plots for wave packet triads for localized variable stratification. Waves constituting each triad has the same order of magnitude of energy. (a) Uniform stratification, (b) localized stratification causing a $\pi/2$ shift, and (c) localized stratification causing π shift.

for the specific example of $\eta = 0$, but for any phase difference η between the waves, if the detuning function introduces a shift of $\pi/2$, the energy transfer will always be different from that of a uniform stratification.

Meanwhile, we can imagine a situation in which the detuning function introduces a phase shift of 2π , in which case there is no difference in energy transfer rates before and after the waves pass through the nonlinear stratification. This is because the waves have the exact relative phase difference. Hence, depending on the amount of the phase shift introduced by the detuning function, a triad (consisting of infinite plane waves or even relatively large width wave packets) may exchange energy similar to a uniform stratification or can be quite different depending upon the initial phase of the three waves (provided they have the same order of magnitude of energy).

Now we focus on a more realistic situation where one wave has at least one order of magnitude higher energy than the other two waves in the triad (to mimic PSI). All the parameters (wavenumbers, angular frequencies, stratification profile) are kept same as the case discussed above. The amplitude profile for the three waves in the triad are given below:

$$a_1 = a_2 = 8 \times 10^{-6} \times e^{-((z-z_c)/S_a)^2} \quad a_3 = 8 \times 10^{-3} \times e^{-((z-z_c)/S_a)^2}.$$

The energy evolution plots are shown in figure 7. It shows that during the initial stages there is little or no effect of the step-like detuning function in the growth of the two daughter wave packets. The results obtained are also independent of initial phases of the daughter wave packets. The same result is also expected to hold true as the wavepackets' size is increased. Hence a localized stratification does not affect the energy transfer for cases where the two daughter waves have much smaller energy than the third (primary) wave.

5. Summary and Conclusion

To summarize, in this paper we have considered triad interactions among internal

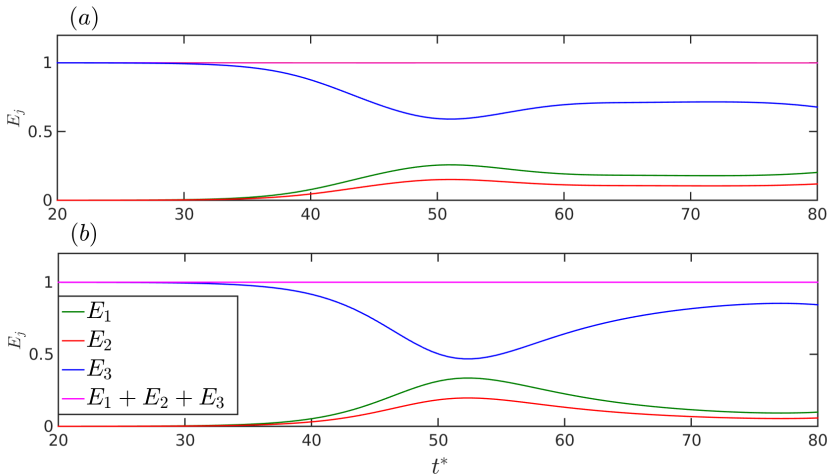


Figure 7: Energy evolution plots for the wave packets: (a) localized stratification, which causes a $\pi/2$ shift, and (b) uniform stratification.

gravity waves whose vertical wavelength is at least an order of magnitude lesser than the pycnocline thickness. Such high wavenumber internal wave triads (or ‘high modes’) significantly influence the energy cascading process that finally leads to ocean turbulence and mixing through PSI. Using a simplified mathematical model, we have studied the energy transfer dynamics in resonant triads in weakly non-uniform stratifications (e.g. the pycnocline region). Although, intuitively one expects very little difference between the energy transfer processes between uniform and weakly non-uniform stratifications, our findings show that the difference is significant. First we use the pump-wave approximation for a near-resonant triad (mismatch in the vertical wavenumber), and then generalize the growth rates of daughter waves for which the amplitude profile of all three waves constituting the triad vary spatially (for simplification, only the z direction is considered). Next we show that the pump-wave approximation, although accurately predicts the growth rate of the daughter waves in a detuned triad, it does not give the complete picture of how much energy was actually transferred. The energy transferred between the waves of a detuned triad and a non-detuned triad may be quite different even for cases where they have same growth rates. Hence pump-wave approximation in near-resonant triads should be used carefully.

We also consider the interaction between wave packets forming a near-resonant (i.e. detuned) triad. It is observed that the mismatch in the vertical wavenumber imposes another constraint on energy transfer between finite wave packets. The near-resonant wave packets need to have a larger width than the resonant wave packets to exchange the same percentage of energy as the resonant wave packets. It is also observed that the near-resonant wave packets have a constraint on the total amount of energy which can be exchanged. For high levels of detuning, increasing the wave packet size didn’t increase the percentage of energy transfer – it reached its saturation level.

Next we considered energy transfer between wave packets in weakly varying stratification. The main factors which influence the energy transfer in such a scenario are:

(i) *Group speed of the wave packets*: Group speed decreases (increases) when wave packets travel to a higher (lower) stratification from a base stratification where the triad conditions are perfectly met.

(ii) *The non-linear coupling coefficients*: These quantities increase (decrease) when

waves packets travel to a higher (lower) stratification from a base stratification where triad conditions are met.

(iii) *Wave detuning*: When wave packets travel to higher stratification from the base stratification (where triad condition is perfectly met), depending on the ratio N^2/ω^2 , the effect of detuning can be strong or weak. Waves packets with $N^2/\omega^2 \approx 1$ are significantly detuned (in vertical wavenumber) even for a small changes in the stratification. This reduces the growth rates of the daughter wave packets. For waves packets satisfying $N^2/\omega^2 \gg 1$, the effect of wave detuning is much weaker than the effect of reduction in group speed or increase in the non-linear coefficients. This results in a significant increase in the growth rates of the wave packets. When the wave packets travel from a base stratification where the triad conditions are met to a lower stratification, the growth rates always decrease.

Appendix A. Scaling analysis for finding the relation between the small parameters

Scaling analysis is performed to predict the relation between the time scale of the amplitude's temporal evolution ($\epsilon_t t$), length scale of the amplitude function ($\epsilon_z z$), and the magnitude of the streamfunction (ϵ_a). The length scale of the amplitude function (a_i) is an input to the system which depends on initial conditions, buoyancy frequency profile, angular frequencies and the vertical wavenumbers of the triad waves. The parameter ϵ_a is decided by the amplitude of the waves which is given in the initial conditions. The streamfunction magnitude of the waves is initialized with values such that the velocity it produces is comparable to realistic conditions.

Let us consider second order wave packet 1's evolution equation (the analysis is similar for all three waves):

$$2i\epsilon_a \left(-m_1\omega_1^2 \frac{\partial a_1}{\partial z} + (k_1^2 + m_1^2)\omega_1 \frac{\partial a_1}{\partial t} + k_1(N^2(\epsilon_n z) - \omega_1^2) \frac{\partial a_1}{\partial x} \right) = \text{RHS} \quad (\text{A } 1)$$

Let us assume that the angular frequencies, horizontal wavenumbers, vertical wavenumbers of all three wave packets are of the same order of magnitude. Therefore, those parameters are respectively scaled with a common angular frequency, horizontal wavenumber and vertical wavenumber. Mathematically:

$$m \sim m_j \quad \omega \sim \omega_j \quad k \sim k_j \quad (\text{A } 2)$$

where ω , k , and m are respectively the scales for angular frequency, horizontal wavenumber and vertical wavenumber of the triad wave packets.

Using the scaling in (A 2), and neglecting the x -direction variation for simplicity, the LHS of (A 1) can be simplified to

$$2i(\epsilon_a) \left(-m_1\omega_1^2 \frac{\partial a_1}{\partial z} + (k_1^2 + m_1^2)\omega_1 \frac{\partial a_1}{\partial t} \right) \sim 2\epsilon_a \left(-m\omega^2 \frac{\partial a}{\partial z} + (k^2 + m^2)\omega \frac{\partial a}{\partial t} \right). \quad (\text{A } 3)$$

In the above equation, the amplitude's evolution with time is assumed to be at least an order lesser than the angular frequency of the wave. Hence the term $\partial a/\partial t$ will scale as: $\partial a/\partial t \sim \epsilon_t \omega$. In a similar way, amplitude's spatial length scale is assumed to be at least an order less than the vertical wavenumber, therefore the term $\partial a/\partial z$ will scale as: $\partial a/\partial z \sim \epsilon_z m$. It is also assumed that the magnitude of the amplitude is a small quantity given separately as ϵ_a . Hence the LHS of (A 3) scales as:

$$\text{LHS} = 2\epsilon_a \left(-m\omega^2 \frac{\partial a}{\partial z} + (k^2 + m^2)\omega \frac{\partial a}{\partial t} \right) \sim 2\epsilon_a \left(-\epsilon_z m^2 \omega^2 + \epsilon_t (k^2 + m^2) \omega^2 \right) \quad (\text{A } 4)$$

The RHS of (A 1) is given by (we ignore the exponential function since it is an $\mathcal{O}(1)$ quantity):

$$\begin{aligned} \text{RHS} = & \left(N^2(k_3 - k_2) \left(-\frac{k_3^2 m_2}{\omega_3} - \frac{k_2^2 m_3}{\omega_2} + \frac{k_3 k_2 m_2}{\omega_2} + \frac{k_3 k_2 m_3}{\omega_3} \right) \left(\frac{m_1}{m_2 m_3} \right)^{1/2} \right) (a_3 \bar{a}_2) \\ & - \left((\omega_3 - \omega_2) ((k_3 m_1 - k_1 m_3) (m_3^2 + k_3^2 - k_2^2 - m_2^2)) \left(\frac{m_1}{m_2 m_3} \right)^{1/2} \right) (a_3 \bar{a}_2). \end{aligned}$$

Using (A 2), the terms in the RHS is found to scale as

$$\text{RHS} \sim m^{2.5} k \omega \epsilon_a^2 \quad (\text{A } 5)$$

Now comparing LHS and RHS respectively obtained from (A 4) and (A 5):

$$2 \left(-\epsilon_z m^2 + \epsilon_t (k^2 + m^2) \right) \omega^2 \epsilon_a \sim (m^{2.5} k) \omega \epsilon_a^2,$$

which on simplification results in

$$-\epsilon_z + \epsilon_t \sim \frac{1}{2} \frac{m^{0.5} k}{\omega} \epsilon_a. \quad (\text{A } 6)$$

The dominant balance can be between any two terms. We mainly focus on three combinations which are given below:

$$\epsilon_t \sim \frac{1}{2} \frac{m^{0.5} k}{\omega} \epsilon_a \quad (\text{A } 7a)$$

$$\epsilon_t \sim \epsilon_z \quad (\text{A } 7b)$$

$$\epsilon_t + \epsilon_z \sim \frac{1}{2} \frac{m^{0.5} k}{\omega} \epsilon_a \quad (\text{A } 7c)$$

In (A 7a), even though the nonlinear terms can be a function of the spatial coordinate z , the equations behave such that z coordinate is a parameter instead of a variable. This is because the term $\partial a / \partial z$ is much smaller than the nonlinear terms. In such kind of systems, detuning in vertical wavenumber will have little or no effect on the growth rates. Similar results was obtained in Craik & Adam (1978), where all three waves have same group speed. In (A 7b), the group speed term is far stronger than the non linear term. In (A 7c), the spatial variation starts to influence the energy transfer (for example, see §3). An important point to note is that in a particular problem, we can decide the approximate value of ϵ_z through the density stratification profile or the wave detuning.

Appendix B. Derivation of the growth rates for (3.4a)–(3.4b)

The governing equations (3.4a)–(3.4b) can be in general written as:

$$\begin{aligned} \frac{\partial \tilde{a}_1}{\partial(\epsilon_t t)} + i G_1 \tilde{a}_1 &= \frac{1}{2} C_1 A_3 \bar{\tilde{a}}_2, \\ \frac{\partial \tilde{a}_2}{\partial(\epsilon_t t)} + i G_2 \tilde{a}_2 &= \frac{1}{2} C_2 A_3 \bar{\tilde{a}}_1. \end{aligned}$$

Here G_1, G_2 are real constants. These two equations can be combined into a single equation, which is given below:

$$\frac{\partial^2 \tilde{a}_2}{\partial(\epsilon_t t)^2} + i(G_1 - G_2) \frac{\partial \tilde{a}_2}{\partial(\epsilon_t t)} + \left(G_1 G_2 - \frac{1}{4} C_1 C_2 A_3^2 \right) \tilde{a}_2 = 0. \quad (\text{B } 2)$$

Let us substitute $a_2(\epsilon t) = e^{-i\Omega t}$ in (B2), where Ω is assumed a complex number and its imaginary part signifies the growth rate. This gives us

$$-\Omega^2 + (G_1 - G_2)\Omega + \left(G_1G_2 - \frac{1}{4}C_1C_2A_3^2\right)\tilde{a}_2 = 0.$$

The roots of the above equation are given by

$$\Omega_{\pm} = \frac{(G_1 - G_2) \pm \sqrt{(G_1 + G_2)^2 - C_1C_2A_3^2}}{2}.$$

Hence the condition for maximum growth rate is $G_1 = -G_2$.

REFERENCES

- BOURGET, B., DAUXOIS, T., JOUBAUD, S. & ODIER, P. 2013 Experimental study of parametric subharmonic instability for internal plane waves. *J. Fluid Mech.* **723**, 120.
- BOURGET, B., SCOLAN, H., DAUXOIS, T., LE BARS, M., ODIER, P. & JOUBAUD, S. 2014 Finite-size effects in parametric subharmonic instability. *J. Fluid Mech.* **759**, 739750.
- VAN DEN BREMER, T. S., YASSIN, H. & SUTHERLAND, B. R. 2019 Lagrangian transport by vertically confined internal gravity wavepackets. *J. Fluid Mech.* **864**, 348380.
- BUSTAMANTE, M. D. & KARTASHOVA, E. 2009 Effect of the dynamical phases on the nonlinear amplitudes' evolution. *Europhys Lett.* **85** (3), 34002.
- CHU, F. Y. F. & SCOTT, A. C. 1975 Inverse scattering transform for wave-wave scattering. *Phys. Rev. A* **12**, 2060–2064.
- CRAIK, A. D. D. 1988 *Wave Interactions and Fluid Flows*. Cambridge University Press.
- CRAIK, A. D. D. & ADAM, J. A. 1978 Evolution in space and time of resonant wave triads. I. The 'pump-wave approximation'. *Proc. Roy. Soc. A* **363** (1713), 243–255.
- DIAMESSIS, P. J., WUNSCH, S., DELWICHE, I. & RICHTER, M. P. 2014 Nonlinear generation of harmonics through the interaction of an internal wave beam with a model oceanic pycnocline. *Dynam. Atmos. Ocean* **66**, 110 – 137.
- ECHEVERRI, P. & PEACOCK, T. 2010 Internal tide generation by arbitrary two-dimensional topography. *J. Fluid Mech.* **659**, 247266.
- GAYEN, B. & SARKAR, S. 2013 Degradation of an internal wave beam by parametric subharmonic instability in an upper ocean pycnocline. *J. Geophys. Res. Oceans* **118** (9).
- GRISOUARD, N., STAQUET, C. & GERKEMA, T. 2011 Generation of internal solitary waves in a pycnocline by an internal wave beam: a numerical study. *J. Fluid Mech.* **676**, 491513.
- HOLBROOK, W. S., FER, I. & SCHMITT, R. W. 2009 Images of internal tides near the Norwegian continental slope. *Geophys. Res. Lett.* **36** (24).
- HUANG, K. M., ZHANG, S. D. & YI, F. 2007 A numerical study on nonresonant interactions of gravity waves in a compressible atmosphere. *J. Geophys. Res. Atmos.* **112** (D11).
- KARIMI, H. H. & AKYLAS, T. R. 2014 Parametric subharmonic instability of internal waves: locally confined beams versus monochromatic wavetrains. *J. Fluid Mech.* **757**, 381402.
- LAMB, K. G. 2004 Nonlinear interaction among internal wave beams generated by tidal flow over supercritical topography. *Geophys. Res. Lett.* **31** (9).
- LAMB, K. G. 2007 Tidally generated near-resonant internal wave triads at a shelf break. *Geophys. Res. Lett.* **34** (18).
- LIGHTHILL, M. J. & LIGHTHILL, J. 2001 *Waves in fluids*. Cambridge university press.
- MATHUR, M., CARTER, G. S. & PEACOCK, T. 2016 Internal tide generation using Green function analysis: To WKB or not to WKB? *J. Phys. Oceanogr.* **46** (7), 2157–2168.
- MC EWAN, A. D. & PLUMB, R. A. 1977 Off-resonant amplification of finite internal wave packets. *Dynam. Atmos. Ocean* **2** (1), 83 – 105.
- MILES, J. W. 1978 The dynamics of the upper ocean, 2nd edition. by O. M. Phillips. Cambridge University Press, 1977. 336 pp. *J. Fluid Mech.* **88** (4), 793794.
- ST. LAURENT, L. & GARRETT, C. 2002 The role of internal tides in mixing the deep ocean. *J. Phys. Oceanogr.* **32** (10), 2882–2899.

- ST. LAURENT, L. & NASH, J. D. 2004 An examination of the radiative and dissipative properties of deep ocean internal tides. *Deep-Sea Res PT II* **51** (25), 3029 – 3042.
- SUTHERLAND, B. R. 2016 Excitation of superharmonics by internal modes in non-uniformly stratified fluid. *J. Fluid Mech.* **793**, 335352.
- VARMA, D. & MATHUR, M. 2017 Internal wave resonant triads in finite-depth non-uniform stratifications. *J. Fluid Mech.* **824**, 286311.
- WUNSCH, S. 2017 Harmonic generation by nonlinear self-interaction of a single internal wave mode. *J. Fluid Mech.* **828**, 630647.